Polymer photovoltaic cells with conducting polymer anodes

Zhang, F.L.; Johansson, M.; Andersson, M.R.; Hummelen, J.C.; Ingan�s, O.; Inganäs, Olle; Inganas, O

Link to publication in University of Groningen/UMCG research database

[20] T. Hellweg, C. D. Dewhurst, E. Bruckner, K. Kratz, W. Eimer, *Colloid Polym. Sci.* **2000**, *278*, 972.

[21] Z. Hu, X. Lu, J. Gao, *Adv. Mater.* **2001**, *13*, 1708.

[22] J. Gao, Z. Hu, *Langmuir* **2002**, *18*, 1360.

[23] R. Pelton, *Adv. Colloid Interface Sci.* **2000**, *85*, 1.

[24] C. D. Jones, L. A. Lyon, *Macromolecules* **2000**, *33*, 8301.

[25] D. Gan, L. A. Lyon, *J. Am. Chem. Soc.* **2001**, *123*, 7511.

[26] D. Gan, L. A. Lyon, *J. Am. Chem. Soc.* **2001**, *123*, 8203.

[27] Y. A. Vlasov, M. Deutsch, D. J. Norris, *Appl. Phys. Lett.* **2000**, *76*, 1627.

[28] It should further be noted that the precision with which the lattice spacing can be tuned should be dependent on one's ability to reproducibly remove controlled solution volumes. Considering the typical accuracy of mechanical pipettes, microliter amounts of water can easily be removed accurately. The average peak shift per microliter for the data shown in Table 1 is ~0.4 nm. We thus calculate that we should be able to tune the interlayer distance by this method with an accuracy that is better than 1.0 nm.

[29] R. Pecora, *Dynamic Light Scattering*, Plenum Press, New York **1985**.

Polymer Photovoltaic Cells with Conducting Polymer Anodes**

By *Fengling Zhang,* Mikael Johansson, Mats R. Andersson, Jan C. Hummelen*, and *Olle Inganäs*

Polymer electronics has become a very attractive field in the last couple of years,[1,2] with applications that include polymer light-emitting diodes (PLEDs), transistors, and photodiodes.[3,4] However, in most cases, polymers are used as active layers, or as thin buffer layers on inorganic conductors such as ITO,[5] and metal electrodes are still routinely used in organic electronic devices. The ambition to develop large area, flexible, and low-cost electronics based on polymer processing and deposition methods is currently being pursued. A prime example of applications for such technology would be found in photovoltaic energy conversion, based on solar energy. Here the main attraction of polymer photovoltaic cells would be found in low processing and materials costs. This should be achieved with a technology that could allow reel-to-reel processing of flexible substrates.

In polymer solar cells, which are rapidly developing and have now reached energy efficiencies of 2.5 %,[6] a layer of transparent indium tin oxide is often used for the anode material. This can be obtained in the form of ITO on a flexible substrate, but it has limited flexibility.

[*] Dr. F. Zhang, Prof. O. Inganäs
Biomolecular and Organic Electronics, IFM, Linköping University
S-581 83 Linköping (Sweden)
E-mail: fenzh@ifm.liu.se

Dr. M. Johansson, Dr. M. R. Andersson
Department of Polymer Technology
Chalmers University of Technology
S-412 96 Göteborg (Sweden)

Prof. J. C. Hummelen
Stratingh Institute, University of Groningen
Nijenborgh 4, NL-9747 AG Groningen (The Netherlands)

Is it possible to use metallic conducting polymers as anodes to completely remove ITO? In many important applications this is clearly not the case. For instance, current densities of 0.01–0.1 A cm^{-2} may be attained in light-emitting diodes (LEDs), resulting in a heavy penalty in the form of a voltage drop in the conducting polymer layer. This problem becomes even more aggravating when it comes to large area devices, such as passive displays based on pulsed driving of a polymer LED pixel, where none of the present day metallic polymers are sufficiently conducting. The situation is somewhat different in the present state of organic and polymer photovoltaic devices. Here, current densities are not expected to ever become larger than ≈0.03 A cm^{-2}, when used for solar energy conversion. The voltage drop in present day thin-film metallic polymers will be excessive, unless current collectors of much higher conductivity are dispersed on the photovoltaic devices surface, in order to make low resistance paths from the photo-generated current to the point of exit. Metallic current collectors are presently used on large-area photovoltaic modules and cells and would be necessary also for coming generations of efficient photovoltaic polymer devices, irrespective of whether ITO or polymer anodes are used. The geometry and patterning of these current collectors may be carried out on different scales, in order to add new functions to the device. The patterning can also be achieved, however, by simple additive techniques on coarse dimensions of the millimeter and the centimeter.

We have investigated the possibility of using thin films of a highly processable polymer complex of poly(3,4-ethylenedioxythiophene) and poly(styrene sulfonate) (PEDOT:PSS) to explore the possibility of using flexible polymer anodes in plastic photovoltaic cells. This material, which can form a uniform transparent thin film on glass or plastics when spin-coated from its odorless, dark blue colored aqueous solution, is widely used in polymer electronic devices as a buffer layer for ITO anodes or metal anodes to improve the performance.[7–9] An advantage of using PEDOT:PSS rather than inorganic metals or oxides is that PEDOT:PSS can be patterned on the micrometer or even nanometer scale by soft-lithography methods[10] to create different device geometries. Our results not only show the possibility of using polymer anodes for photodiodes, but they also constitute a simple approach to fabricating other organic electronics devices. Here, we report on PEDOT:PSS and "enhanced" PEDOT:PSS as anodes in photovoltaic cells.

The preparation of the PEDOT:PSS anodes is described in the Experimental section. On the top of the PEDOT:PSS layer, two active layers were spin-coated. The first layer is a semiconducting polymer—here we use a high molecular weight MEH-PPV (poly(2-methoxy, 5-(2′-ethyl-hexyloxy)-1,4-phenylene vinylene)) as the electron donor layer. The second layer consists of a fullerene derivative [6,6]-phenyl-C$_{61}$-butyric acid methyl ester (PCBM)[11,12] as an electron acceptor. The sequential spin-coating from hot xylene (Merck) for MEH-PPV and room temperature xylene for PCBM leaves a stratified bilayer, in which the concentrations

of the polymer and the acceptor vary continuously throughout the thickness of the organic layer.[13] Finally, aluminum (Al; 60 nm) is deposited as cathode, by vapor deposition, and so the sandwich structure of photovoltaic cells is anode/MEH-PPV/PCBM/Al (see Fig. 1). The sizes of the active area in these diodes are 5–7 mm^2. The devices were prepared without using a protective atmosphere.
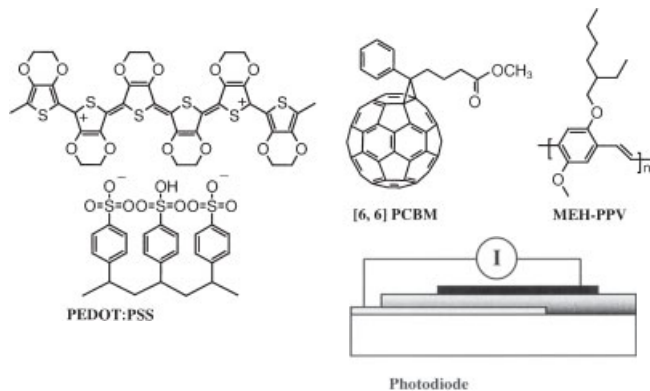

Fig. 1. The molecular structures of PEDOT:PSS, MEH-PPV, and PCBM as well as the structure of the photodiodes.

To compare the performance of these cells to traditional devices, we fabricated several identically structured photovoltaic cells, but with different anodes. The anodes were: ITO (Merck, 20 Ω/square), normal PEDOT:PSS (~1.5 × 10^5 Ω/square), PEDOT:PSS doped with glycerol (PEDOT:PSS:G) and PEDOT:PSS doped with sorbitol (PEDOT:PSS:S)—the latter two typically with surface resistances of 10^3 Ω/square—and normal PEDOT:PSS on top of ITO (ITO/PEDOT:PSS).

The performance of these cells was measured under ambient conditions using the reported setup.[14] The cells were illuminated using low intensity monochromatic light, and the photocurrents were recorded as a function of the wavelength of the light. The external quantum efficiencies (EQEs) of these cells are shown in Figure 2a. It can be seen that the EQE of cells with polymer anodes is comparable to the cell with only ITO as an anode.

The I–V characteristics of these diodes under monochromatic light ($\lambda = 530$ nm; 0.12 mW cm^{-2}), are shown in Figure 2b (symbols corresponding to those for the diodes in Figure 2a). The photovoltages of diodes made with normal PEDOT:PSS, doped PEDOT:PSS, and ITO/PEDOT:PSS anodes are higher than that of the diode on ITO. The monochromatic fill factor (FF) and energy conversion efficiencies (ECEs) of these diodes are listed in Table 1, together with the anode resistances (measured with a four point probe), short circuit current (I_{sc}), and open circuit voltage (V_{oc}). The ECE of all diodes is of the same order of magnitude, indicating that diodes on the various PEDOT:PSS anodes are as good as the diode on ITO under low-intensity monochromatic illumination.

However, when the incident light intensity was increased by about three orders of magnitude, that is, when these diodes were illuminated by simulated solar light (AM1.5; 78 mW cm^{-2}), the I–V curves show that the photocurrents in the diode
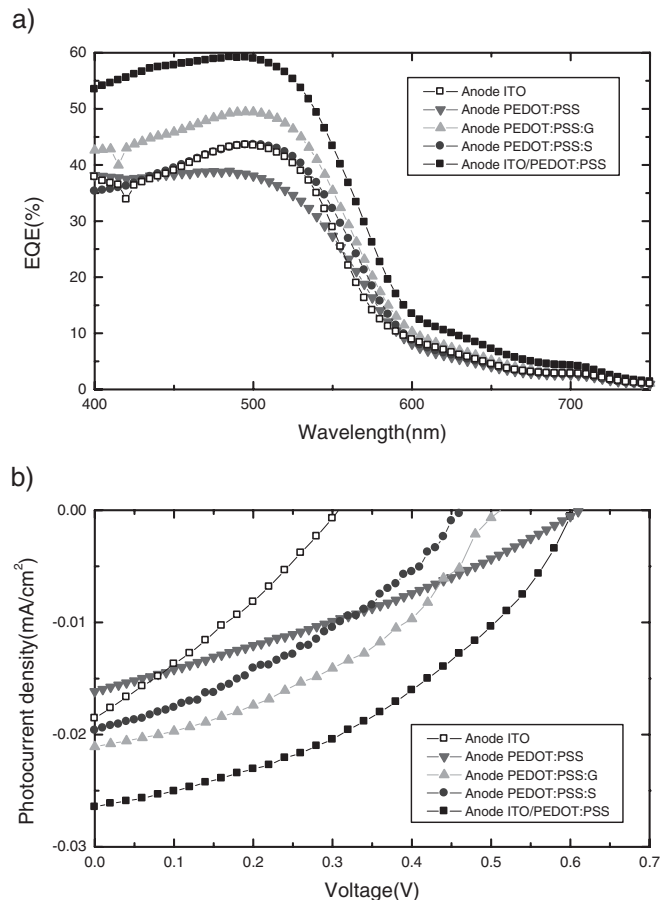

Fig. 2. a) EQE of photodiodes with different anode materials: with ITO anode (□); with PEDOT:PSS anode (▼); with PEDOT:PSS:G anode (▲); with PEDOT:PSS:S anode (●); with ITO/PEDOT:PSS anode (■). b) I–V characteristics of photodiodes with different anode materials: with ITO anode (□); with PEDOT:PSS anode (▼); with PEDOT:PSS:G anode (▲); with PEDOT:PSS:S anode (●); with ITO/PEDOT:PSS anode (■).

Table 1. The performances of glass/anode/MEH-PPV/PCBM/Al photodiodes with different anode materials under monochromatic light (530 nm, 0.12 mW cm^{-2})

Anode	Resistance of anodes [Ω/sq]	I_{sc} [mA/cm^2]	V_{oc} [V]	FF_{max}	η [%]
ITO	~20	1.9×10^{-2}	0.30	0.30	1.4
PEDOT:PSS	~1.5×10^5	1.6×10^{-2}	0.61	0.31	2.6
PEDOT:PSS:G	~1.3×10^3	2.1×10^{-2}	0.47	0.40	3.4
PEDOT:PSS:S	~1.0×10^3	2.0×10^{-2}	0.46	0.36	2.8
ITO/PEDOT:PSS	~20	2.6×10^{-2}	0.60	0.41	5.4

on PEDOT:PSS and the diode on PEDOT:PSS:G are respectively one order of magnitude and two times lower than that of the other three diodes (Fig. 3). Only the photocurrent produced by the diode on PEDOT:PSS:S compares with that of the diode on ITO and the diode on ITO/PEDOT:PSS. The resistance of PEDOT:PSS becomes significant in the diode on PEDOT:PSS and the diode on PEDOT:PSS:G at intense illumination, which is reflected in a much lower photocurrent flow, even though the photovoltages are still higher than that of the diode on ITO. A comparison of performance of these
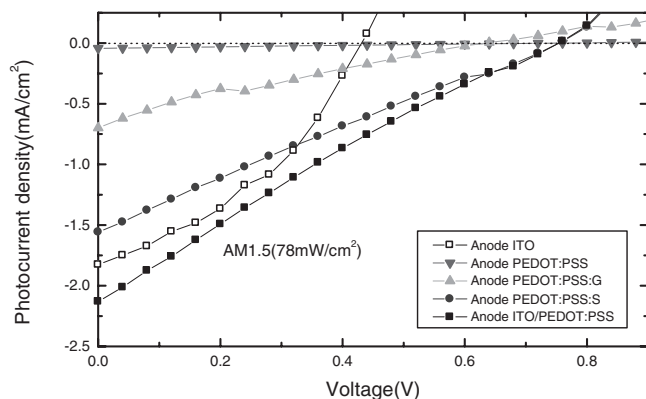
Fig. 3. *I–V* characteristics of photovoltaic cells with different anodes under AM1.5 illumination: with ITO anode (□); with PEDOT:PSS anode (▼); with PEDOT:PSS:G anode (▲); with PEDOT:PSS:S anode (●); with ITO/PEDOT:PSS anode (■).

diodes under AM1.5 conditions is shown in Table 2. Under these conditions, the best anode material is ITO/PEDOT:PSS, the second best is ITO, the third is PEDOT:PSS:S, the fourth is PEDOT:PSS:G, and the worst material in our series is normal PEDOT:PSS. The performance of ITO and PEDOT:PSS:S is close, indicating that PEDOT:PSS doped with sorbitol can be used as anode instead of ITO for photovoltaic cell applications in cases where ITO is not suitable.

Table 2. The performances of glass/anode/MEH-PPV/PCBM/Al photovoltaic cells with different anode materials under simulated solar light (AM1.5; 78 mW cm^{-2})

Anode	I_{sc} [mA/cm^2]	V_{oc} [V]	FF_{max}	η [%]
ITO	1.8	0.43	0.38	0.39
PEDOT:PSS	0.044	0.74	0.24	0.01
PEDOT:PSS:G	0.70	0.63	0.22	0.12
PEDOT:PSS:S	1.6	0.75	0.24	0.36
ITO/PEDOT:PSS	2.1	0.75	0.23	0.46

Materials for anodes in photovoltaic cells require high transparency, high conductivity, and a suitable work function. The optical transmission spectra of the anodes used in this investigation are similar and quite flat in the visible range. The transmission of the five anodes is over 80 % in the wavelength range 350–600 nm at thicknesses of 150–200 nm, and the transmission of PEDOT:PSS, PEDOT:PSS:G, and PEDOT:PSS:S becomes roughly 10 % lower than that of ITO only at wavelengths above 600 nm. This would only become a limiting factor when low bandgap materials are used as active layer constituents.

However, there are clear differences in the conductivity and work function of ITO and PEDOT:PSS. Our results indicate that the different conductivity does not influence the performance of these diodes under low-intensity illumination, i.e., at low current density. Under high-intensity illumination, however, the performance of diodes becomes limited by the conductance of electrodes. Yet, even under high illumination, the diode based on PEDOT:PSS doped with sorbitol as the anode performed comparably to the ITO-based device.

The open circuit voltage of devices under high-intensity illumination according to Malliaras et al.[15] depends on the work function difference between the two electrodes. We note that our devices show a photovoltage increase with an increase in work function difference, i.e., when the anode is changed from ITO to PEDOT:PSS. With increasing difference in work functions, V_{oc} becomes larger. The work function of Al is 4.2 eV, that of PEDOT is 5.2 eV,[16] and that of ITO is 4.5–5.14 eV.[17] Therefore, the V_{oc} in devices based on ITO anodes will always be smaller than in devices based on PEDOT:PSS anodes (see Tables 1 and 2). From this point of view, PEDOT is better than ITO as an anode in photodiodes, which partly compensates for its high resistance.

When photodiodes are used as imaging detectors, pixel formation and electric addressing of pixels is necessary. Therefore, from the view point of easy and low cost electric addressing in organic devices, a polymer anode has a clear advantage over the ITO anode in terms of processing and patterning. The inclusion of a Cu current collector[18] with proper patterning[19] for minimal light obstruction may be a choice both for arrays of photodiodes and for solar cells.

In conclusion, we have evaluated the possibility of substituting ITO by a conducting polymer PEDOT:PSS and its doped forms (PEDOT:PSS:G and PEDOT:PSS:S) as the transparent anodes in photovoltaic cells. Our results show that it is feasible to use processable conducting (macro)molecular materials instead of ITO for fabricating polymer photovoltaic cells, with the potential to obtain lower cost and more mechanically flexible devices.

Experimental

To prepare the anodes for our photodiodes, the conducting polymer PEDOT:PSS (Baytron P, Bayer AG) mixed with glycerol (ALDRICH, 99+ %) or sorbitol (SIGMA, D-sorbitol, >98 %) was spin-coated on a cleaned glass. The reason for mixing the PEDOT:PSS with glycerol or sorbitol is that the conductivity of the polymer can be increased by two orders of magnitude (to ~10^3 S m^{-1}), by doping with glycerol or sorbitol followed by heat treatment [20], as measured by four point probe after annealing. The optimum conductivity occurs when PEDOT:PSS is mixed with 85 wt.-% glycerol, then heated at 140 °C or with 65 wt.-% sorbitol, to convert the film at 190 °C, for 20 s in air in both cases. There might be glycerol and sorbitol left in the films after conversion. The thicknesses of polymer anodes are 150 nm for doped PEDOT:PSS and 200 nm for normal PEDOT:PSS, as measured with a Sloan Dektak 3030 surface profilometer. The surface resistances of PEDOT:PSS doped with glycerol and sorbitol are of the same order of magnitude. The resistance of PEDOT:PSS doped with glycerol (1300 $\Omega \text{ sq}^{-1}$) is a little higher than that of PEDOT:PSS doped with sorbitol (1000 $\Omega \text{ sq}^{-1}$).

The optical transmission spectra of the various PEDOT:PSS and ITO layers on a glass substrate were measured with a Perkin Elmer λ9 spectrophotometer.

[1] M. Granström, M. Berggren, D. Pede, O. Inganäs, M. R. Andersson, T. Hjertberg, O. Wennerstrom, *Supramol. Sci.* **1997**, *4*, 27.
[2] J. Bharathan, Y. Yang, *Appl. Phys. Lett.* **1998**, *72*, 2660.
[3] W. R. Salaneck, M. Lögdlund, *Polym. Adv. Technol.* **1998**, *9*, 419.
[4] A. J. Salih, J. M. Marshall, J. M. Maud, *Philos. Mag. Lett.* **1997**, *75*, 169.
[5] A. J. Campbell, D. D. C. Bradley, H. Antoniadis, *Synth. Met.* **2001**, *122*, 161.
[6] S. E. Shaheen, C. J. Brabec, N. S. Sariciftci, *Appl. Phys. Lett.* **2001**, *78*, 841.

[7] M. Granström, M. Berggren, O. Inganäs, *Science* **1995**, *267*, 1479.
[8] C. S. Wang, M. Kilitziraki, L. O. Palsson, M. R. Bryce, A. P. Monkman, I. D. W. Samuel, *Adv. Funct. Mater.* **2001**, *11*, 47.
[9] A. C. Arias, M. Granström, K. Petritsch, R. H. Friend, *Synth. Met.* **1999**, *102*, 953.
[10] T. Granlund, T. Nyberg, L. S. Roman, M. Svensson, O. Inganäs, *Adv. Mater.* **2000**, *12*, 269.
[11] O. Inganäs, L. S. Roman, F. L. Zhang, D. M. Johansson, M. R. Andersson, J. C. Hummelen, *Synth. Met.* **2001**, *121*, 1525.
[12] G. Yu, J. Gao, J. C. Hummelen, F. Wudl, A. J. Heeger, *Science* **1995**, *270*, 1789.
[13] L. C. Chen, D. Godovsky, O. Inganäs, J. C. Hummelen, R. A. J. Janssens, M. Svensson, R. Andersson, *Adv. Mater.* **2000**, *12*, 1367.
[14] L. A. A. Pettersson, L. S. Roman, O. Inganäs, *J. Appl. Phys.* **1999**, *86*, 487.
[15] G. G. Malliaras, J. R. Salem, P. J. Brock, J C. Scott, *J. Appl. Phys.* **1998**, *84*, 1583.
[16] G. Greczynski, T. H. Kugler, W. R. Salaneck, *Thin Solid Films* **1999**, *354*, 129.
[17] J. S. Kim, B. Lägel, E. Moons, N. Johansson, I. D. Baikie, W. R. Salaneck, R. H. Friend, F. Cacialli, *Synth. Met.* **2000**, *111*, 315.
[18] L. S. Roman, O. Inganäs, T. Granlund, T. Nyberg, M. Svensson, M. R. Andersson, J. C. Hummelen, *Adv. Mater.* **2000**, *12*, 189.
[19] L. S. Roman, *Ph.D. Thesis*, Linkoping University, Sweden **2000**.
[20] M. Krogh, unpublished.

Fabrication of High-Density, High Aspect Ratio, Large-Area Bismuth Telluride Nanowire Arrays by Electrodeposition into Porous Anodic Alumina Templates**

By *Melissa S. Sander, Amy L. Prieto, Ronald Gronsky,** Timothy Sands*, and *Angelica M. Stacy*

Wires with diameters of a few tens of nanometers or less are attracting considerable fundamental and technological interest because of their unique properties relative to the bulk. The properties of nanowires can be harnessed for a variety of applications, for example those requiring high current or redundancy, in dense arrays consisting of parallel wires. While several nanowire array fabrication methods have been developed, template-based approaches are well suited for producing arrays with uniform diameters and high aspect ratio wires.[1–4] In particular, porous anodic alumina templates have many desirable characteristics, including tunable pore dimensions over a wide range of diameters (~7–300 nm) and lengths (to >100 μm), good mechanical and thermal stability, and well-developed fabrication methods.[5–8] In this work, we have

[*] Prof. R. Gronsky, Prof. T. Sands
Department of Materials Science & Engineering
University of California, Berkeley
Berkeley, CA 94720 (USA)
E-mail: rgronsky@socrates.berkeley.edu
M. S. Sander,[+] A. L. Prieto, Prof. A. M. Stacy
Department of Chemistry, University of California, Berkeley
Berkeley, CA 94720 (USA)
[+] Current address: Institute of Materials Research and Engineering, 3 Research Link, 117602, Singapore.

employed anodic alumina templates to fabricate nanowire arrays of Bi_2Te_3, which have potential applications in thermoelectric devices due to the predicted enhanced thermoelectric properties of nanowires relative to the bulk.[9,10] We have deposited nanowire arrays by electrochemical deposition, which offers advantages over other deposition methods because it ensures electrically continuous wires and enables good control over stoichiometry. We describe a method to produce high-density (~5×10^9 cm^{-2}), high aspect ratio (>1000), uniform, narrow diameter (45 nm ± 5 nm) Bi_2Te_3 nanowire arrays over large areas (>1 mm^2). This fabrication methodology may be applied to produce a wide range of both elemental and compound nanowire array systems.

There have been several previous reports of nanowire array fabrication by DC electrodeposition into porous anodic alumina templates;[11–16] however, there has been little emphasis on producing thick, dense, large-area templates suitable for facile assessment of the array properties over a homogeneous composite structure and potential incorporation into device structures. The fabrication of nanowire arrays with these characteristics is difficult due to the extremely narrow diameter, high aspect ratio pores, as well as the fragility of the templates. In previous reports, DC electrodeposition into alumina templates was used to produce nanowires by first fabricating a freestanding template and subsequently depositing an electrode layer for electrodeposition. In recent work, we used this technique to fabricate Bi_2Te_3 nanowire arrays with a high degree of wire nucleation (in >80 % of the pores) and complete pore filling in ~10–20 % of the pores.[17] In the new fabrication approach reported here, several processing steps that lead to template damage or contamination have been eliminated, allowing reproducible fabrication of dense arrays with high aspect-ratio wires over large areas.

A schematic of the method employed to fabricate the nanowire arrays is shown in Figure 1. In this approach, first, one surface of an Al foil is mechanically polished, the thermal oxide layer is chemically removed, and a Ag film is sputter-deposited onto the Al to serve as an electrode in subsequent electrochemical deposition. Then, the Al is anodized to produce a nanoporous alumina template for nanowire array fabrication. The Al foil is prepared for anodization by mechanical polishing followed by electrochemical polishing in a method adapted from previous work.[18] After anodization, the template is transferred to an aqueous solution for Bi_2Te_3 nanowire electrodeposition. Before electrodeposition, the template is allowed to soak for approximately one to two hours at room temperature in the 1 M HNO_3 solution in order to dissolve the barrier layer at the base of the pores (this step also causes slight pore widening). The oxide barrier layer in films prepared by anodization on the Ag substrate is thinner than in films prepared in aluminum, which allows for removal of the barrier layer without simultaneous dissolution of the entire anodic film.[19] We employ the deposition parameters for producing highly crystalline, textured, stoichiometric thin films of Bi_2Te_3 established in prior work.[20–22] At the beginning of the deposition, the template becomes nearly uni-